

We are IntechOpen, the world's leading publisher of Open Access books Built by scientists, for scientists

6,900

Open access books available

186,000

International authors and editors

200M

Downloads

Our authors are among the

154

Countries delivered to

TOP 1%

most cited scientists

12.2%

Contributors from top 500 universities



WEB OF SCIENCE™

Selection of our books indexed in the Book Citation Index
in Web of Science™ Core Collection (BKCI)

Interested in publishing with us?
Contact book.department@intechopen.com

Numbers displayed above are based on latest data collected.
For more information visit www.intechopen.com



Coastal Morphological Modeling

Yun-Chih Chiang¹ and Sung-Shang Hsiao²

¹*Tzu Chi University,*

²*National Taiwan Ocean University
Taiwan*

1. Introduction

The coastal zone is the area where the action of waves and wave-driven-currents on the seabed is very intense, and where the bed level and sediment are almost always in motion. If the mainly seasonal climate changes, the wind and wave conditions will also change. A new waves and wave-driven-currents conditions will change the rate of sediment transport and the beach topography. Natural beaches are significant characterized by an annual cycle of seasonal erosion and accretion. In other words, natural beaches are generally in dynamic equilibrium from the balance of sediment transport budget for specific area on the beach. We can utilize the conservation law of sediment transport to describe the coastal morphodynamic evolution. It is the same way to predict beach evolution due to changes in wave conditions or caused by coastal structures. Therefore, we can utilize numerical models to predict the change of bottom topography from the spatial distribution of the alongshore and offshore sediment transport rates in real coastal area.

Coastal morphological models are indispensable and powerful tools that allow harbour and hydraulic engineers to predict nearshore topography, to analyze the impact of coastal structures, and to verify the planning and design of harbours and coastal defences. Morphological models are based on various sub-models for waves, tidal currents, nearshore currents, and sediment transport, coupled with the sediment transport model. The sediment transport model solves the sediment conservation equation to calculate bed-level evolution. The local sediment transport is first calculated by wave and current sub-models, and the bed form evolution is then computed based on the conservation of sediment and its continual redistribution in time. The aim of this chapter is to describe the theories, techniques, applications and robust algorithms for computing bed level change which is flexible enough to handle the nonlinearity present in the sediment conservation equations describing bed evolution in a complex coastal area.

1.1 Classification of prediction methods for morphological evolution

The changes of coastal topography were the complex and irreversible morphodynamic processes, influenced by local bathymetry, weather, wave, tide, and coastal structures, etc. The technology of prediction morphological evolution caused by coastal structures or varied with monsoon, typhoon, and climate changes, etc. is needed. In order to predict morphological evolutions, the experience analysis with many survey data in similar cases and the results of hydraulic model tests are considered in the past.

The empirical morphodynamic analysis was based on observed trends of coastal evolution with a series of sequential bathymetry survey data or present trends under similar geographic and natural conditions. This prediction method should take a lot of times and resources to complete. However, the prediction with empirical analysis cannot be applied widely with general coastal areas subjecting to specific condition in similar case.

Hydraulic modeling analysis is a well established and widely accepted fact among the coastal engineering professionals that the physical hydraulic scale model test is not only a choice but an reliable tool for testing coastal structures before its construction due to its ability to solve complex hydraulic problems which otherwise cannot be solved analytically or experience morphological analysis. However, model tests for coastal morphodynamic evolution involve scaling problems such as sediment particle hardly scaling down and similitude law for coastal movable bed tests not well established. Furthermore, hydraulic model tests usually have been studied with expensive facilities, laboratory resource and time.

In recent years, computer technology has made remarkable progress and a computer has become an indispensable tool for coastal morphodynamic analysis. Upon the deficiencies of the empirical morphological analysis and hydraulic model tests, the numerical model simulation is a convenient, economical and efficient tool for analyzing coastal morphodynamic evolution. In order to predict coastal morphological evolution, the coastal processes must be understood, appropriately simplified, and mathematically modelling. Numerical simulations for long-term (years to decades) periods and wide coastal area should be different from short-term (hours to days) and medium-term (weeks, months to years). According to the objective and simplified mathematic formulation of numerical modelling, the coastal morphological models can be classified into two general groups: the shoreline models (single-line or multi-line model) and three-dimensional models.

The shoreline model is a numerical prediction model based on the cross-shore-section sediment continuity equation and an equation for the longshore sediment transport rate. It is also called the one-line theory for the prediction of beach position changes, where the 'one-line' refers to the shoreline. The two-line and multi-line models have also been developed to calculate the movement of selected contours. The shoreline models, which have been well developed and applied to many practical problems, simplified the actual phenomena, and hence require only a relatively shore computation time, but they cannot be used to predict local changes in the bottom topography.

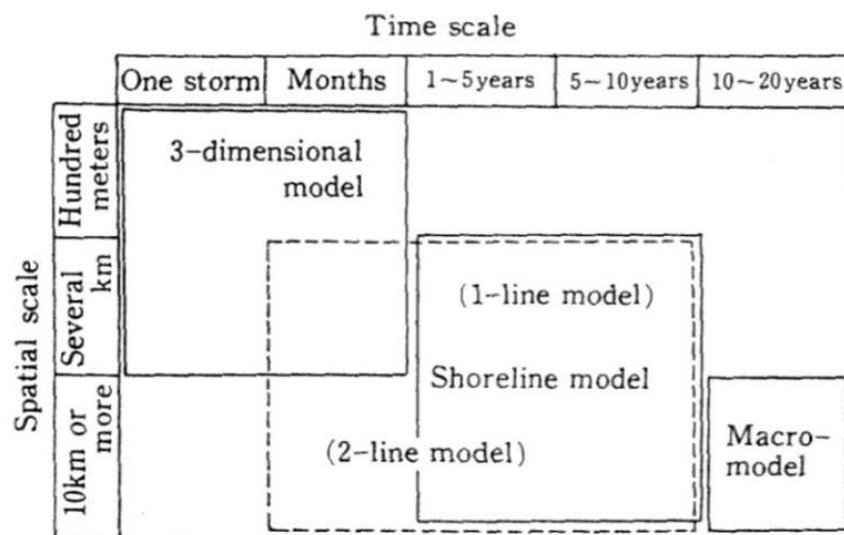


Fig. 1.1 Application ranges of morphological evolution predictive models. (Horikawa, 1986)

The three-dimensional models are used to predict the changes of bed level and bottom topography from spatial distributions of the sediment transport rates in cross-shore and longshore direction, which are estimated with the results of nearshore wave and current simulation. Compared with the shoreline models, the three-dimension models of coastal topography changes don't require more simplification and idealizations. On the other hand, the three-dimension models could be applied to analyze local coastal topography changes and therefore they have wider applicability, but a long computation time is required. However, the deficiencies of much computation time have been overcome with remarkable progress in computer techniques. Therefore, the three-dimension models of coastal topography changes could be applied with predicting local bed level changes in bottom topography over short-term and middle-term time interval.

According to Horikawa (1986), Figure 1.1 indicates criteria of application ranges of coastal morphological evolution models in terms of time scales and spatial scales. The macro-models in the figure denote the more simplified empirical morphological analysis based on similar evolution trend experience and a lot of local survey data, and they are effective for a qualitative analysis but not applicability to quantitative analysis.

1.2 The main concern of coastal morphological models in present chapter

Coastal morphological models are indispensable and powerful tools that allow harbour and hydraulic engineers to predict nearshore topography, to analyze the impact of coastal structures, and to verify the planning and design of harbours and coastal defences. Morphological models are based on various sub-models for waves, tidal currents, nearshore currents, and sediment transport, coupled with the sediment transport model. The sediment transport model solves the sediment conservation equation to calculate bed-level evolution. The local sediment transport is first calculated by wave and current sub-models, and the bed form evolution is then computed based on the conservation of sediment and its continual redistribution in time. In the last twenty years, two dimensional depth-averaged coastal morphological models have been developed, and these models have been applied in the short-term (hours to days) and medium-term (weeks, months to years) (Coffe' and Pe'chon, 1982; Yamaguchi and Nishioka, 1984; Watanabe, 1986; Anderson et al., 1991; Wang et al., 1992; de Vriend et al., 1993b; Sato et al, 1995; Nicholson et al., 1997)

2. Modelling coastal morphological evolution

2.1 Conservation of sediment transport

The change of bed form in local bottom elevation z_b can be computed by solving the conservation equation for sediment mass. In two dimensions, this can be written as:

$$\frac{\partial}{\partial t} \left[(1-n)z_b + \int_{z_b}^{\eta} cdz \right] + \left(\frac{\partial q_x}{\partial x} + \frac{\partial q_y}{\partial y} \right) = 0 \quad (1)$$

where z_b is the bed level elevation, defined as positive up from a fixed datum, x and y are horizontal space coordinates, t is time, n is the bed porosity, η is the free surface elevation, c is the suspended sediment concentration in the water column per unit area, and q_x and q_y are the total volumetric sediment transport rates (unit: m^3/sec) in the x - and y - directions, as shown in Figure 2.1, respectively. The sediment transport rates are expressed in terms of the effective volume of sediment passing through the vertical cross-section of unit width in unit

time. The effective volume means the volume consisted of sediment particles included voids by the changes of bed level in the unit area. If the income of sediment transport rates is larger than outcome, the sediment effective volume will settle on the bottom and increase the bed level. If the outcome of sediment transport rates is larger than income, the bed form will be washed out to follow mass conservation law. Therefore, in applying Eq. (1) it should be noted that the changes in bed level is caused by net averaged sediment transport affected with the wave and current field.

In general, the suspended load contribution of sediment can be consisted in sediment flux, and the sediment transport conservation equation can be reduced to:

$$\frac{\partial z_b}{\partial t} + \frac{1}{1-n} \left(\frac{\partial q_x}{\partial x} + \frac{\partial q_y}{\partial y} \right) = 0 \quad (2)$$

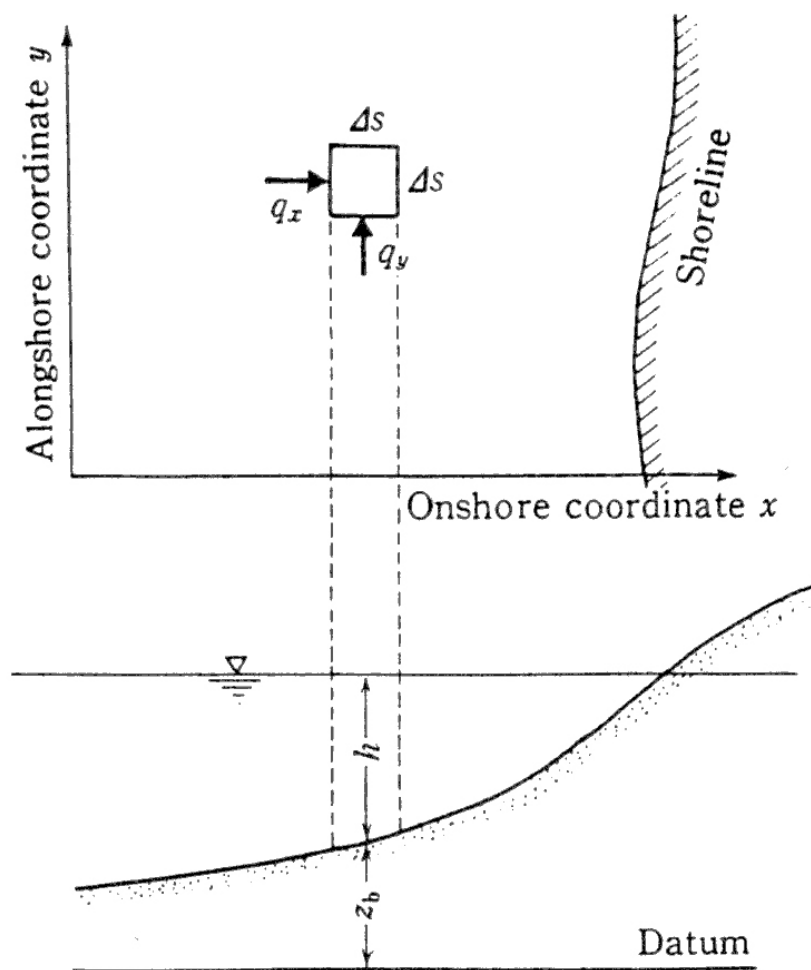


Fig. 2.1 The definition of coordination.

The sediment transport rates q_x and q_y are complex functions of several parameters, including waves, currents, water depth, density, and sediment properties (including grain size and porosity). Here, we assume the sediment properties and water level are fixed in every time step. Under these assumptions, the sediment transport rates caused by waves and currents can

be calculated using the formula obtained through experimentation or theory. At present, no established and widely accepted formulas are available for estimating local sediment transport rates from local coastal quantities while general wave and current conditions.

Therefore, the most important problem is how to quantify the sediment transport rates caused by waves and currents. There are many studies on sediment transport formulas have been reviewed in previous chapters. However, there is no universally acceptable and reliable sediment transport formulas have been found for accurately evaluating the local sediment transport rates everywhere without local data verification. For following simulation examples, the experimental results of alongshore and offshore transport rate for following simulation examples suggested by Chiang et al. (1996), which is applicable for Taiwan coastal areas are employed:

$$q_x = q_c(u + U_r) \quad (3)$$

$$q_y = q_c(v + V_r) \quad (4)$$

$$q_c = \left\{ A_1 f_c \left[(u + U_r)^2 + (v + V_r)^2 \right] + A_2 (U_w^2 - U_{wc}^2) \right\} / g \quad (5)$$

$$U_w = \sqrt{\frac{\tau_m}{\rho}} = \sqrt{\frac{f_w}{2}} \times U_{w\max}, \quad U_{w\max} = \frac{\pi H}{T \sinh(kh)} \quad (6)$$

$$U_{wc} = 8.41 \times d_{50}^{11/32} \quad (7)$$

$$f_c = g / C_c^2 \quad (8)$$

$$f_w = \begin{cases} 0.00251 \times \exp \left(5.21 \times \exp \left(\frac{A}{k_s} \right)^{-0.19} \right), & \frac{A}{k_s} > 1.57 \\ 0.3, & \frac{A}{k_s} \leq 1.57 \end{cases} \quad (9)$$

$$A = \frac{H}{2} \sinh(kh) \quad (10)$$

where u and v are the depth integrated average current velocity in the x - and y - directions, respectively; U_r and V_r are the average equivalent river flow velocity in the x - and y - directions; A_1 and A_2 are the coefficients of sediment transport due to currents and waves; f_c and f_w are the friction factors for mean current and wave orbital fluid motion; U_w and $U_{w\max}$ are the shear velocity and its maximum velocity due to wave motion; U_{wc} is the critical shear velocity for the inception of particle motion; g is the gravitational acceleration; C_c is the non-dimensional Chezy coefficient; d_{50} is the median grain diameter; A is the semi-orbital excursion; H is the wave height; T is the wave period; k is the wave number; and h is the water depth.

2.2 Sample computation and discussions

In the example of coastal morphological models, the morphological evolution in the vicinity of a shore parallel breakwater is investigated from Johnson and Zyserman (2002) using

MIKE 21 CAMS (The same governing equation and similar sediment transport formula as below). The test conditions are described below.

A shore parallel breakwater 310 m long is placed at a distance of 360 m from the shoreline. The initial bathymetry is characterised by a 1:50 plane beach profile to a depth of 14 m, and a 1:20 plane beach slope to the boundary of the model area (depth of 20 m). Irregular unidirectional waves with $H_{rms} = 1.98$ m and $T_p = 8.0$ s propagate towards the coast from $167.5^\circ N$ at a water depth of 20 m. The normal to the beach points towards the south ($180^\circ N$). The flow of water along the coast is driven only by wave action.

The sand characteristics are specified as $D_{50} = 0.20$ mm and $(D_{84}/D_{16})^{0.5} = 1.40$ everywhere along the coast. The porosity of the bed material is taken as 40%. The model area covers an area of 2700×840 m (alongshore extent \times offshore extent). This model setup is the same as test KM3 of Zyserman et al. (1998), with different sediment properties.

In this example, a maximum morphological time step of 1 hour is specified. The wave field is updated every 3 hours (or every third morphological step), and the morphological simulation carried out for 14 days. The computed bathymetry is shown in Fig. 2-2.

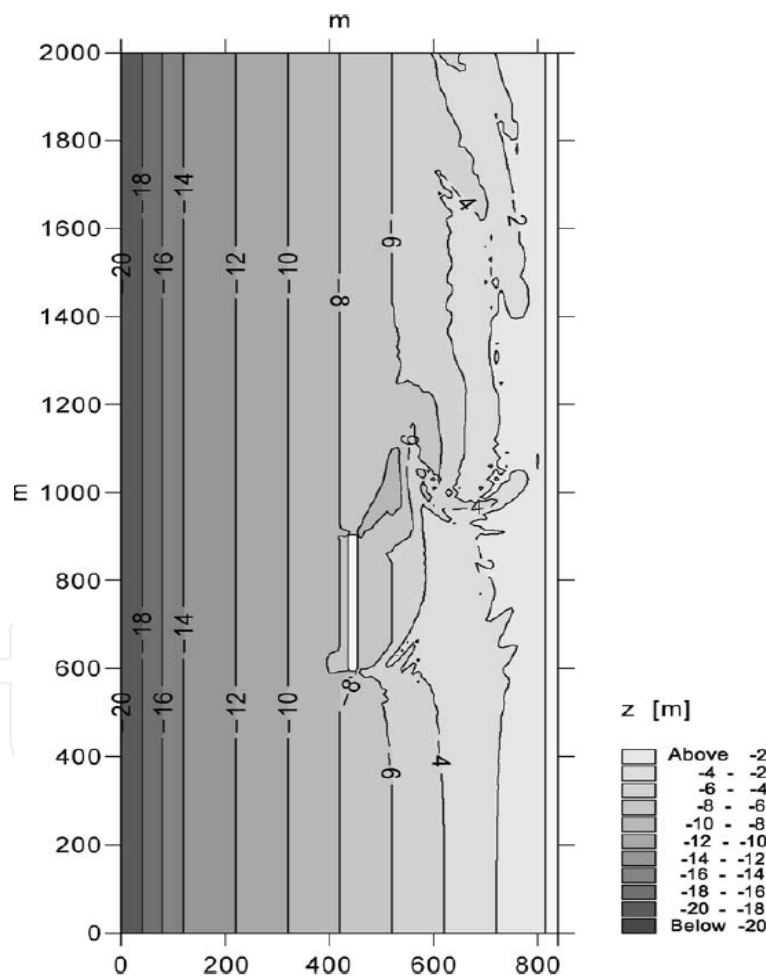


Fig. 2.2 Morphological evolution in the vicinity of a detached breakwater. Computed bathymetry after 14 days. (Johnson and Zyserman, 2002)

Fig. 2.2 shows the general features of the morphological evolution after 14 days. Some oscillatory salient had formed in the lee of the breakwater. A tendency for unsteady erosion

at the down drift edge of the breakwater can also be observed. In addition, high wave number spatial oscillations of the bottom contours can also be observed at several sections. In the example of Johnson and Zyserman (2002), the morphological simulation is completed by MIKE 21 CAMS, the wave simulation is carried out using MIKE 21 PMS, the flow simulations using MIKE 21 HD and the sand transport calculations using MIKE 21 ST. However, MIKE PMS and HD are one of the state-of-art numerical model for evaluating wave and current field, and perform well in many studies. Why the unsteady results appeared? According to Johnson and Zyserman (2002), the origin of spatial oscillations in numerical morphological models is traced to the dependence of the bed celerity with bed levels, which is due to the non-linear relationship between sediment transport and bed levels.

In these morphodynamic systems as shown in sec. 1.2, the governing equations are a nonlinear function of bed level. The sediment transports, which are caused by waves and currents, are also calculated from complicated nonlinear hydrodynamic systems. The nonlinear couplings and numerical scheme errors in these sub-models can generate unstable and inaccurate numerical results, whose natures are still poorly understood. Even though the results of all sub-models are accurate and robust, their combination in the sediment conservation equation also leads to numerical oscillations and instabilities (Jensen et al. 1999). They generally fail to accurately predict the bed form evolution in surf zone and in the areas around coastal structures for long term simulations (Johnson and Zyserman 2002). Several techniques to improve accuracy and stability for coastal morphological modeling have been developed in the last decades. The main concern of these studies is to stabilize the solutions when solving the sediment conservation equation. As reviewed in Long et al. (2008), many state-of-the-art models introduce oscillation controlling schemes for bed form evolution modeling. The Delft Hydraulics model Delft2D-MOR (Roelvink et al. 1994 and 1998) utilizes a forward time, central space explicit scheme with a corrected sediment transport rate to offset the negative diffusion terms in the scheme. The University of Liverpool model (O'Connor and Nicholson, 1995, Nicholson et al. 1997) uses a two-step Lax-Wendroff scheme considering the effects of gravity on the bed slope for sediment transport rates. Vincent and Caltagirone (1999) also use a modified Lax-Wendroff scheme with the Total Variation Diminishing scheme (LW-TVD) and a slope limiter. Cayocca (2001) uses a forward-time upwind scheme with the transport rate corrected due to the effect of the bed form slope (de Vriend, 1987a,b) and an input filtering technique (de Vriend et al., 1993a,b)[10, 11] to prevent oscillation. Johnson and Zyserman (2002) illustrate that the bed form slope plays a principal role in the instability of morphological numerical schemes and expands a second order Taylor-Series of the bed level in time: the first order time derivative term is composed of the sediment conservation equation calculated with the Lax-Wendroff scheme, and the second order time derivative term is regarded as the diffusion terms of advection equation. Their morphological scheme is also modified with a low-pass filter to dissipate spurious high frequency oscillations (suggested by Jensen et al., 1999). Saint-Cast (2002) applied the high-resolution NOC (Non-Oscillating Centered) scheme (based on Jiang and Tadmor, 1998) and bedform slope updating technique (suggested by Watanabe, 1988) to solve the sediment conservation equation without a filter or limiter. Shao et al. (2004), Long et al. (2008) and Chiang et al. (2010) utilized the WENO (Weighted Essentially Non-Oscillatory) algorithm from the Computational Fluid Dynamics scheme (based on Liu et al., 1994 and Jiang et al., 1999) to solve the 1D and 2D sediment conservation equation without any filters or limiters.

In order to perform well to calculate the change in coastal topography for long term simulations under waves and wave-driven currents, the model should not only be able to control the oscillations in space, but also improve the accuracy in time. The model should also take into account the effects caused by the discontinuity of the contours and beach slopes.

There are two points to be noted. First, the simulating oscillations of coastal morphological evolution should be recognized. The second point is, which techniques of controlling oscillations perform well? We will discuss in next sub-section and next section.

2.3 Analysis of oscillations for morphological scheme

As mentioned in the Introduction, several works have focused on controlling oscillations of coastal morphological schemes. Watanabe (1988), Cayocca (2001), Johnson and Zyserman (2002) suggested modifying the conservation equation to consider bottom elevation changes. Following Watanabe (1988), it is apparent that the sediment grains tend to move downward due to the distribution force of gravity, while the local slope becomes steep; the effect of bottom slope should be taken into account. Although the simulation of the wave-current field by hydraulic models varies with the beach transformation, the change of the sediment transport flux alone cannot be expected to completely suppress the creation of a jagged bed form profile. Modification of sediment transport rate was suggested as (Watanabe, 1988):

$$q_x = q_{x0} - \varepsilon_s |q_{x0}| \frac{\partial z_b}{\partial x} \quad (11)$$

$$q_y = q_{y0} - \varepsilon_s |q_{y0}| \frac{\partial z_b}{\partial y} \quad (12)$$

Where ε_s is a positive diffusivity constant; the value of which will be determined empirically. The second subscript "0" indicates sediment transport on a flat bottom.

It is noted that Watanabe (1988) did not consider the influence of the cross-slope terms in the alongshore direction, but they should be included for complex bathymetries. Johnson and Zyserman (2002) suggested including the cross-slope terms:

$$q_x = q_{x0} - \varepsilon_{xx} |q_{x0}| \frac{\partial z_b}{\partial x} - \varepsilon_{xy} |q_{x0}| \frac{\partial z_b}{\partial y} \quad (13)$$

$$q_y = q_{y0} - \varepsilon_{yy} |q_{y0}| \frac{\partial z_b}{\partial y} - \varepsilon_{yx} |q_{y0}| \frac{\partial z_b}{\partial x} \quad (14)$$

where ε_{xx} , ε_{xy} , ε_{yy} , and ε_{yx} are also positive diffusivity constants.

We substitute Eqs. (12), (13) into Eq. (2), to obtain:

$$\begin{aligned} \frac{\partial z_b}{\partial t} + \frac{1}{1-n} \left(\frac{\partial q_{x0}}{\partial z_b} \frac{\partial z_b}{\partial x} + \frac{\partial q_{y0}}{\partial z_b} \frac{\partial z_b}{\partial y} \right) &= \frac{\partial}{\partial x} \left[\frac{\varepsilon_{xx} |q_{x0}| \partial z_b}{(1-n) \partial x} \right] + \\ &+ \frac{\partial}{\partial y} \left[\frac{\varepsilon_{yy} |q_{y0}| \partial z_b}{(1-n) \partial y} \right] + \frac{\partial}{\partial x} \left[\frac{\varepsilon_{xy} |q_{x0}| \partial z_b}{(1-n) \partial y} \right] + \frac{\partial}{\partial y} \left[\frac{\varepsilon_{yx} |q_{y0}| \partial z_b}{(1-n) \partial x} \right] \end{aligned} \quad (15)$$

We can rewrite Eq. (15) as an advection-diffusion equation of bed form elevation:

$$\begin{aligned} \frac{\partial z_b}{\partial t} + C_{x0} \frac{\partial z_b}{\partial x} + C_{y0} \frac{\partial z_b}{\partial y} = & \frac{\partial}{\partial x} \left[\left(\frac{\varepsilon_{xx} |q_{x0}|}{1-n} \right) \frac{\partial z_b}{\partial x} \right] + \frac{\partial}{\partial y} \left[\left(\frac{\varepsilon_{yy} |q_{y0}|}{1-n} \right) \frac{\partial z_b}{\partial y} \right] + \\ & + \frac{\partial}{\partial x} \left[\left(\frac{\varepsilon_{xy} |q_{x0}|}{1-n} \right) \frac{\partial z_b}{\partial y} \right] + \frac{\partial}{\partial y} \left[\left(\frac{\varepsilon_{yx} |q_{y0}|}{1-n} \right) \frac{\partial z_b}{\partial x} \right] \end{aligned} \quad (16)$$

where

$$C_{x0} = \frac{1}{1-n} \frac{\partial q_{x0}}{\partial z_b} \quad C_{y0} = \frac{1}{1-n} \frac{\partial q_{y0}}{\partial z_b}$$

The right-hand side of Eq. (16) represents the diffusion terms. These terms show that the effect of bed slope and the value of transport rates play an important role as diffusion parameters. The stability of the morphological scheme is based on these diffusion terms under control. Consequently, these diffusivity constants ε_{xx} , ε_{xy} , ε_{yy} , and ε_{yx} should be chosen carefully and sediment transport rates in Eqs. (13) and (14) should be updated in every time step after the new bed elevation is computed.

Long et al. (2008), Hsu and Hanes (2004), and Henderson et al. (2004) address the appearance of wave phase-resolving sediment transport models for nearshore applications by waves and wave-driven nearshore currents. Because the wave orbital fluid motion is oscillatory in space and time, the resulting sediment transport fluxes should also be oscillatory. Unfortunately, there are no schemes that can be applied to solve the advection-diffusion conservation equation while removing the effect of the oscillation by wave orbit motion without any limiters or artificial viscosities. Chiang et al. (2010) recommend the application of numerical oscillation removal techniques with the simulation of bed form evolution by solving the conservation equation of sediment under wave motions and wave-driven currents, such as bed-slope feedback, oscillation and the removal in spatial and temporal discretization. The details of these techniques are shown in the following sections.

3. Modification of coastal morphological models

More recently, the advantages and disadvantages of these controlling oscillatory morphological models were reviewed. Several numerical schemes are reviewed by Callaghan et al. (2006), including a first order upwind scheme, two Lax-Wendroff schemes (Vincent and Caltagirone, 1999 and Johnson and Zyserman, 2002) and the NOC scheme (Saint-Cast, 2002). Long et al. (2008) review two Lax-Wendroff schemes (based on the Richtmyer scheme and the MacCormack scheme) and three WENO schemes (the TVD-RK-WENO scheme by Shao et al., 2004, the Euler-WENO scheme by Long et al., 2008 and Bed-level updated two-steps three-time-levels WENO scheme by Chiang et al., 2010). According to these reviewed results, Lax-Wendroff schemes or modified Lax-Wendroff schemes for morphodynamic system are not stable for long term simulation of bed level evolution. The filter, limiter, or artificial viscosity should be added to prevent numerical oscillation in these schemes. They also found that it is difficult to determine the phase celerity of the bed form, which is the most important parameter for the scheme's stability, when these weakened morphological schemes are applied to complex bathymetry. These powerful oscillations removal techniques will be introduced after.

3.1 Feedback by bed-slope updating scheme

As mentioned before, the morphodynamic system to be calculated when coupling the hydrodynamic (waves and wave-driven currents) and sediment transport into the morphological models (governed by conservation equation of sediment) is inherently unstable. This highly non-linear system will lead to diffusion if the effect of bed-slope variations in time is not taken into account (Watanabe, 1988; de Vriend et al., 1993a, b). In the morphological model, the linear stability analysis of bed-level and quasi-steady conditions for waves and currents are assumed. The waves and currents are assumed to remain unchanged during the entire calculation period, while the bathymetry does vary. Under this assumption, the sediment transport rates obtained from waves and currents remains unchanged over the same time duration. Even though the wave orbital velocity and current velocity remain unchanged, the bed level changes at every time step. This inconsistency implies that some quantities related to bed level, such as the friction factor and the sediment transport direction factor will also change.

In order to modify sediment transport with bed form slope, the down slope gravitational transport rate is the most commonly utilized while the bed-level changes are greater than a threshold value (Watanabe 1988; Maruyama and Takagi, 1988; de Vriend et al., 1993a, and b; Cayocca 2001; Anunes do Carmo and Seabra-Santos, 2002). Consequently, the conservation equation of sediment mass coupled with the bed-slope updated terms in two-dimensions can be rewritten as:

$$\frac{\partial z_b}{\partial t} + \frac{\partial}{\partial x} \left(q_{x0} - \varepsilon_{xx} |q_{x0}| \frac{\partial z_b}{\partial x} - \varepsilon_{xy} |q_{x0}| \frac{\partial z_b}{\partial y} \right) + \frac{\partial}{\partial y} \left(q_{y0} - \varepsilon_{yy} |q_{y0}| \frac{\partial z_b}{\partial y} - \varepsilon_{yx} |q_{y0}| \frac{\partial z_b}{\partial x} \right) = 0 \quad (17)$$

Chiang et al. (2010) recommend that the modified bed-slope feedback should be processed at every time step. It is very effective for the removal oscillations for long term simulations.

3.2 Controlling oscillations in spatial discretization

In order to control the oscillations in space for the morphological model, there are several numerical schemes as reviewed by Callaghan et al. (2006) and Long et al. (2008). Among these oscillation removal schemes, the NOC and WENO scheme are more stable finite-difference schemes than the others.

3.2.1 NOC (Non-Oscillating Centered) scheme

NOC scheme is a general non-oscillating scheme originally developed by Nessyahu and Tadmor (1990) and extended to 2D by Jiang and Tadmor (1998). It solves multidimensional hyperbolic fluid conservation equations using a staggered grid method, again directly utilizing fluxes. It is similar to be applied with sediment conservation equation, and directly using sediment fluxes is good for avoiding the estimation of characteristic bedform velocity. The examples of NOCS applications for coastal area include linear oblique advection, the two-dimensional Burger and Euler equations and the one-dimensional shallow water wave equations (Williams and Peregrine, 2002). Their approach uses two staggered grids, which are moving the calculated results from one grid to another half grid with every time step. However, the staggered grid system, while minimizing scheme diffusion is impractical for morphological models consisting of a looped arrangement of individual components for sediment transport caused by waves and currents. According to Saint-Cast (2002), there is an extension of the original scheme where the new solution was initially determined on the

staggered grid and then reconstructed on the original grid (Jiang et al., 1998). This extension is easily integrated into looped morphological models for the NOC scheme.

The NOC scheme was first applied for coastal morphological modeling by Saint-Cast (2002) with the purpose of explaining ridge and runnel formation on sand beaches exposed to consistent north Atlantic swells. The work by Saint-Cast (2002) included initial testing against analytical solutions and simulations of an idealized crescent shape barred beach evolutions. Callaghan et al. (2006) utilize the NOC scheme with an idealized river entrance, perpendicular to a straight beach with constant slope, under waves and currents and show its stability by comparison with other schemes.

3.2.2 WENO (Weighted Essentially Non-Oscillatory) scheme

The WENO schemes are based on the essentially non-oscillatory (ENO) schemes, which were first developed by Harten et al. (1987) in the form of finite volume schemes and were later improved by Shu and Osher (1988). The ENO schemes are generalizations of the total variation diminishing (TVD) schemes of Harten (1983). The TVD schemes are designed so that the total variation of specific quantity in space remains constant or only decrease in time. During the solution process, there will be no new extrema generated. In other words, the TVD schemes typically degenerate to first-order accuracy at locations with smooth extrema, while the ENO schemes maintain high-order accuracy. The key idea of the ENO schemes is to use the smoothest stencil among several candidates to approximate the fluxes at the cell boundaries to high order and at the same time to avoid spurious oscillations near shocks and discontinuities. The WENO schemes process one step further by taking a weighted average of all candidates, and the weights are adjusted by the local smoothness.

The first version of WENO schemes was developed by Liu et al. (1994) for one-dimensional conservation laws of fluid mechanics. Jiang and Shu (1996) applied the scheme to multi-dimensional cases with a new weighting procedure to obtain optimized accuracy. Later, Jiang and Wu (1999) extended a high-order (5th) accurate WENO finite difference scheme, which has successfully attained comparable accuracy with fewer time-steps in computations. Shao et al. (2004) first applies the WENO scheme to solve the one-dimensional conservation equation of sediment mass and study the evolution of periodic sand bars in the presence of waves at the resonant Bragg frequency. Long et al. (2008) use the Euler-WENO schemes, based on first order explicit time discretization with the WENO scheme, to study the evolution of periodic alternating sand bars in a rectangular open channel with gravity flow. Chiang et al. (2010) applied the bed-slope feedback, 3 levels 2 time-steps, WENO morphological scheme to calculate topography changes of complex coastal area under waves and currents, and found that the stability was performed very well. The full detail of the WENO scheme applied with coastal morphological modeling can be found in Chiang et al. (2010).

The key of inaccuracy of numerical morphological modeling is to obtain the characteristic phase velocity of bedform variation to modified sediment fluxes. Fortunately, another advantage of WENO scheme is that split sediment fluxes only involve the sign of characteristic bedform velocity instead of accurate calculations. Based on the accuracy of algorithm, the fifth order WENO scheme is recommended in this chapter.

3.2.3 Controlling oscillatory morphological models with WENO scheme

In this subsection, we briefly present the finite difference version for the sediment conservation equation (Eq. (2)) using the WENO schemes. Following the numerical

algorithms of Jiang et al. (1998) and the assumption of Long et al. (2008), we will describe the one-dimensional problem first, and then extend to two-dimensions. To achieve numerical stability and to avoid entropy-violating solutions, upwinding and sediment flux splitting approaches are used. The sediment transport rate can be split into two parts associated with bedform propagation in the positive and negative x (offshore) directions. This can be written as:

$$q(C) = q^+(C) + q^-(C) \quad (18)$$

$$q^+ = (1-n) \int_0^{z_b} C^+(z) dz \quad (19)$$

$$q^- = (1-n) \int_0^{z_b} C^-(z) dz \quad (20)$$

where C is phase velocity of the bedform and C^+ and C^- are the phase velocities of the bedform propagating in the positive and negative x -directions, respectively, i.e. $C^+ = \max(C, 0)$, $C^- = \min(C, 0)$. Thus,

$$\frac{dq^+(C)}{dC} \geq 0, \text{ for } C = C^+ \quad (21)$$

$$\frac{dq^-(C)}{dC} \leq 0, \text{ for } C = C^- \quad (22)$$

Following Jiang and Wu (1999), the WENO scheme uses a conservative approximation to the spatial derivatives,

$$\frac{\partial z_b}{\partial t} = -\frac{\partial q}{\partial x} = -\frac{\hat{q}_{i+1/2} - \hat{q}_{i-1/2}}{\Delta x} \quad (23)$$

where $\hat{q}_{i+1/2}$ and $\hat{q}_{i-1/2}$ are the approximations of the sediment transport rate at grid locations $(i+1/2)$ and $(i-1/2)$, respectively, for the three stencil system of the WENO scheme (Fig. 3.1).

We then apply the WENO approximation procedure, as was given in Eq. (18), to obtain two numerical fluxes, $\hat{q}_{i+1/2}^\pm$, and sum them to obtain the numerical flux $\hat{q}_{i+1/2}$:

$$\hat{q}_{i+1/2} = \hat{q}_{i+1/2}^- + \hat{q}_{i+1/2}^+ \quad (24)$$

The left-biased-flux $\hat{q}_{i+1/2}^-$ of Eq. (24) is calculated by the WENO scheme with approximations of three sub-stencils in a five point stencil system (grid positions from $i-2$ to $i+2$ in Fig. 1). The idea of the WENO scheme is to properly weight the three sub-stencils for the five points. This is written as:

$$\hat{q}_{i+1/2}^- = \begin{cases} \omega_0 q_{i+1/2}^0 + \omega_1 q_{i+1/2}^1 + \omega_2 q_{i+1/2}^2, & C_{i+1/2} \geq 0 \\ 0, & C_{i+1/2} < 0 \end{cases} \quad (25)$$

where ω_s ($s = 0, 1, \text{ or } 2$) are the positive weights, and $q_{i+1/2}^s$ ($s=0, 1, \text{ or } 2$) are the approximations of the sub-stencils.

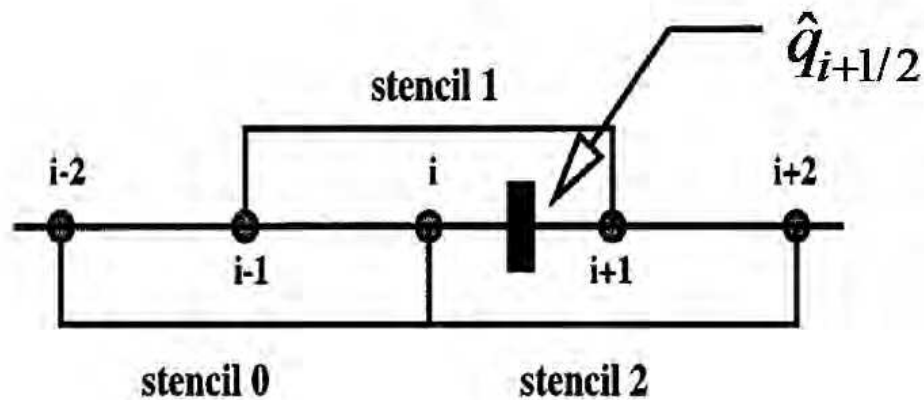


Fig. 3.1 The three sub-stencils with five points of WENO approximation

In each sub-stencil s ($s=0, 1, \text{ or } 2$), the 3rd-order accurate approximation $q_{i+1/2}^s$ is obtained by the Taylor series expansion as:

$$q_{i+1/2}^0 = \frac{1}{3}q_{i-2} - \frac{7}{6}q_{i-1} + \frac{11}{6}q_i \quad (26)$$

$$q_{i+1/2}^1 = -\frac{1}{6}q_{i-1} + \frac{5}{6}q_i + \frac{1}{3}q_{i+1} \quad (27)$$

$$q_{i+1/2}^2 = \frac{1}{3}q_i + \frac{5}{6}q_{i+1} - \frac{1}{6}q_{i+2} \quad (28)$$

The WENO scheme procedure of three sub-stencils with the five point system possesses the following properties in Eq. (25): (1) the approximation $\hat{q}_{i+1/2}$ at grid position $i+1/2$ is accurate to the fifth-order; and (2) no Gibbs phenomena occur (i.e., spurious oscillations), while $\hat{q}_{i+1/2}$ is discontinuous near $i+1/2$.

In accordance with the above two properties, Jiang and Shu (1996) suggested the calculation of weights as:

$$\omega_0 = \frac{\alpha_0}{\alpha_0 + \alpha_1 + \alpha_2} \quad (29)$$

$$\omega_1 = \frac{\alpha_1}{\alpha_0 + \alpha_1 + \alpha_2} \quad (30)$$

$$\omega_2 = \frac{\alpha_2}{\alpha_0 + \alpha_1 + \alpha_2} \quad (31)$$

where the coefficients $\alpha_0, \alpha_1, \alpha_2$ are calculated by Long et al. (2008) :

$$\alpha_0 = \frac{0.1}{(\varepsilon + IS_0)^2} \quad (32)$$

$$\alpha_1 = \frac{0.6}{(\varepsilon + IS_1)^2} \quad (33)$$

$$\alpha_2 = \frac{0.3}{(\varepsilon + IS_2)^2} \quad (34)$$

In which $\varepsilon \approx 10^{-20}$ is used to prevent the denominators of Eqs. (32) - (34) from becoming zero, and the smoothness measurements are written as:

$$IS_0 = \frac{13}{12}(a-b)^2 + \frac{1}{4}(a-3b)^2 \quad (35)$$

$$IS_1 = \frac{13}{12}(b-c)^2 + \frac{1}{4}(b+c)^2 \quad (36)$$

$$IS_2 = \frac{13}{12}(c-d)^2 + \frac{1}{4}(3c-d)^2 \quad (37)$$

Where

$$a = q_{i-2} - q_{i-1} \quad (38)$$

$$b = q_{i-1} - q_i \quad (39)$$

$$c = q_i - q_{i+1} \quad (40)$$

$$d = q_{i+1} - q_{i+2} \quad (41)$$

Similarly, we can give the right-biased-flux $\hat{q}_{i+1/2}^+$ of Eq. (24) in the same procedure.

$$\hat{q}_{i+1/2}^+ = \begin{cases} \tilde{\omega}_0 \tilde{q}_{i+1/2}^0 + \tilde{\omega}_1 \tilde{q}_{i+1/2}^1 + \tilde{\omega}_2 \tilde{q}_{i+1/2}^2, & C_{i+1/2} < 0 \\ 0, & C_{i+1/2} \geq 0 \end{cases} \quad (42)$$

with

$$\tilde{q}_{i+1/2}^0 = -\frac{1}{6}q_{i-1} + \frac{5}{6}q_i + \frac{1}{3}q_{i+1} \quad (43)$$

$$\tilde{q}_{i+1/2}^1 = \frac{1}{3}q_i + \frac{5}{6}q_{i+1} - \frac{1}{6}q_{i+2} \quad (44)$$

$$\tilde{q}_{i+1/2}^2 = \frac{11}{6}q_{i+1} - \frac{7}{6}q_{i+2} + \frac{1}{3}q_{i+3} \quad (45)$$

$$\tilde{\omega}_0 = \frac{\tilde{\alpha}_0}{\tilde{\alpha}_0 + \tilde{\alpha}_1 + \tilde{\alpha}_2} \quad (46)$$

$$\tilde{\omega}_1 = \frac{\tilde{\alpha}_1}{\tilde{\alpha}_0 + \tilde{\alpha}_1 + \tilde{\alpha}_2} \quad (47)$$

$$\tilde{\omega}_2 = \frac{\tilde{\alpha}_2}{\tilde{\alpha}_0 + \tilde{\alpha}_1 + \tilde{\alpha}_2} \quad (48)$$

$$\tilde{\alpha}_0 = \frac{0.1}{(\varepsilon + I\tilde{S}_0)^2} \quad (49)$$

$$\tilde{\alpha}_1 = \frac{0.6}{(\varepsilon + I\tilde{S}_1)^2} \quad (50)$$

$$\tilde{\alpha}_2 = \frac{0.3}{(\varepsilon + I\tilde{S}_2)^2} \quad (51)$$

$$I\tilde{S}_0 = \frac{13}{12}(b-c)^2 + \frac{1}{4}(b-3c)^2 \quad (52)$$

$$I\tilde{S}_1 = \frac{13}{12}(c-d)^2 + \frac{1}{4}(c+d)^2 \quad (53)$$

$$I\tilde{S}_2 = \frac{13}{12}(d-e)^2 + \frac{1}{4}(3d-e)^2 \quad (54)$$

$$b = q_{i-1} - q_i \quad (55)$$

$$c = q_i - q_{i+1} \quad (56)$$

$$d = q_{i+1} - q_{i+2} \quad (57)$$

$$e = q_{i+2} - q_{i+3} \quad (58)$$

At the grid location $i-1/2$, the left-biased-flux $\hat{q}_{i-1/2}^-$ can be repeated using Eqs. (24) - (58) by simply shifting i backward one grid. Consequently, the spatial discretization of WNEO finite difference scheme for one-dimensional sediment conservation problem is complete. With a simple 1st-order forward temporal discretization, Eq. (2) can be solved by the Euler-WENO scheme as:

$$\frac{z_{bi}^{n+1} - z_{bi}^n}{\Delta t} + \frac{1}{1-n} \frac{\hat{q}_{i+1/2} - \hat{q}_{i-1/2}}{\Delta x} = O(\Delta t, \Delta x^5) \quad (59)$$

The extension of the Euler-WENO scheme for Eq. (2) in two-dimensions can be easily given as:

$$\frac{z_{bi,j}^{n+1} - z_{bi,j}^n}{\Delta t} + \frac{1}{1-n} \frac{\hat{q}_{i+1/2,j}^n - \hat{q}_{i-1/2,j}^n}{\Delta x} + \frac{1}{1-n} \frac{\hat{q}_{i,j+1/2}^n - \hat{q}_{i,j-1/2}^n}{\Delta y} = O(\Delta t, \Delta x^5, \Delta y^5) \quad (60)$$

3.2.4 Phase celerity of the bedform

There is only one undetermined parameter for the bed-level updated WENO scheme; namely the phase celerity of the bed form. Eq. (2) can be written as:

$$\frac{\partial z_b}{\partial t} + \frac{1}{1-n} \left(\frac{\partial q_x}{\partial z_b} \frac{\partial z_b}{\partial x} + \frac{\partial q_y}{\partial z_b} \frac{\partial z_b}{\partial y} \right) = 0 \quad (61)$$

Since the phase velocity of bedforms can be assumed as $C_x = 1 / (1-n) \partial q_x / \partial z_b$, $C_y = 1 / (1-n) \partial q_y / \partial z_b$, Eq. (61) becomes:

$$\frac{\partial z_b}{\partial t} + C_x \frac{\partial z_b}{\partial x} + C_y \frac{\partial z_b}{\partial y} = 0 \quad (62)$$

In order to calculate the phase celerity C_x and C_y , Eq. (66) can be written in vector form and Eq. (2) is substituted into it:

$$\vec{C} = \frac{-\frac{\partial z_b}{\partial t}}{|\nabla z_b|^2} \vec{\nabla} z_b = \frac{\vec{\nabla} \cdot \vec{q}}{(1-n)|\nabla z_b|^2} \vec{\nabla} z_b \quad (63)$$

where vector $\vec{C} = (C_x, C_y)$, $\vec{q} = (q_x, q_y)$.

For one-dimensional case, Eq. (63) is reduced to:

$$C(z_b) = \frac{\frac{\partial q}{\partial x}}{(1-n) \frac{\partial z_b}{\partial x}} \quad (64)$$

We can calculate the phase celerity of the bedform by solving Eq. (63) and (64) for one- and two-dimensional problems. Hudson et al. (2005) suggested a central difference scheme to calculate the phase celerity for the one-dimensional case:

$$C_i = \frac{q_{i+1} - q_{i-1}}{(1-n)(z_{bi+1} - z_{bi-1})} \quad (65)$$

There are some disadvantages when applying Eq. (65) to estimate phase celerity in a real coastal area. It fails when $z_{bi+1} = z_{bi-1}$, and causes significant errors when the central difference spatial grid spans sand bars, dunes, or ripples. Fortunately, the WENO scheme only requires the sign of the bedform phase celerity for split sediment transport. Long et al. (2008) suggested a simple formula to calculate the sign of the phase celerity:

$$\text{sign}(C_i) = \text{sign}((q_{i+1} - q_i)(z_{bi+1} - z_{bi})) \quad (66)$$

3.3 Controlling oscillations in temporal discretization

As mentioned before, the inaccuracy of bed-level simulation in every time-step is caused by discretization errors and oscillation factors from the sub-models of waves, currents, or sediment transport rates. They will lead to diffusions and dispersions in the long term. There are three typical techniques for controlling oscillations in temporal discretization as following.

3.3.1 Explicit two-step, three-time-level finite difference scheme

In this subsection, the explicit two-step, three-time-level finite difference scheme with stagger grid is introduced (Chiang et al., 2010). This technique can be easily implemented in time discretization and does not lead to a significant CPU time increases. The gradient of sediment fluxes is expanded at half grid position and the bed-level is calculated at original grid position. It is convenient to apply the operator of WENO scheme with approximated sediment fluxes. For one-dimensional sediment conservation problem, Eq. (2) becomes:

Step 1.

$$\frac{z_{bi}^{n+1/2} - z_{bi}^n}{\Delta t / 2} + \frac{1}{1-n} \frac{\hat{q}(q_0, z_{bi}^n)_{i+1/2} - \hat{q}(q_0, z_{bi}^n)_{i-1/2}}{\Delta x} = 0 \quad (67)$$

Step 2.

$$\frac{z_{bi}^{n+1} - z_{bi}^n}{\Delta t} + \frac{1}{1-n} \frac{\hat{q}(q_0, z_{bi}^{n+1/2})_{i+1/2} - \hat{q}(q_0, z_{bi}^{n+1/2})_{i-1/2}}{\Delta x} = 0 \quad (68)$$

where the $\hat{q}(\)$ is the operator of WENO scheme. This scheme gives 2nd order accuracy $O(\Delta t^2)$ in time.

3.3.2 TVD-Runge-Kutta scheme

TVD (Total Variation Diminishing) schemes are designed such that the total variance of the solution $TV = \int_{-\infty}^{+\infty} |\partial z_b / \partial x| dx$ will remain constant or only decrease in time. During the solution process, there will be no new extrema generated. TVD scheme were often proposed based on existing schemes. Shu and Osher (1988) and Shao et al. (2004) applied a TVD-Runge-Kutta (TVD-RK) scheme for 3rd order time integration of Eq. (2). The TVD-RK scheme can be summarized as an algorithm of 5 steps:

The 1st step consists of an Euler forward step to get time level n+1:

$$\frac{1}{\Delta t} (z_b^{n+1} - z_b^n) + \frac{\partial}{\partial x} \left(\frac{1}{1-n} q(z_b^n) \right) = 0 \quad (69)$$

The 2nd step uses a second forward step to time level n+2:

$$\frac{1}{\Delta t} (z_b^{n+2} - z_b^{n+1}) + \frac{\partial}{\partial x} \left(\frac{1}{1-n} q(z_b^{n+1}) \right) = 0 \quad (70)$$

The 3rd step uses an averaging step to obtain an approximation solution at $n+1/2$:

$$z_b^{n+1/2} = \frac{3}{4}z_b^n + \frac{1}{4}z_b^{n+2} \quad (71)$$

The 4th step uses a 3rd Euler step to get time level $n+3/2$:

$$\frac{1}{\Delta t} \left(z_b^{n+3/2} - z_b^{n+1/2} \right) + \frac{\partial}{\partial x} \left(\frac{1}{1-n} q \left(z_b^{n+1/2} \right) \right) = 0 \quad (72)$$

the 5th step uses another averaging step finally to get solution at time level $n+1$:

$$z_b^{n+1} = \frac{1}{3}z_b^n + \frac{2}{3}z_b^{n+2/3} \quad (73)$$

3.3.3 Predictor-corrector method

As mention before, instability problems appear to originate from the explicit discretization of the sediment conservation equation, Fortunato and Oliveira (2007) recommend a predictor-correct scheme was implemented and performed well. It is shown as below:

Predictor step: an estimate of depth at time $n+1$ is first calculated as:

$$h^{(p)} = h^n + \frac{1}{1-n} \nabla \int_n^{n+2} q(u(t), \eta(t), h^n) dt \quad (74)$$

Corrector step: a fully or semi-implicit scheme is applied with the correction step as:

$$h^{n+1} = h^n + \frac{1}{1-n} \nabla \int_n^{n+2} q(u(t), \eta(t), h^*) dt \quad (75)$$

where h is depth, $h^* = ah^{(p)} + (1-a)h^n$, a is the implicitness parameter in $[0,1]$. Eqs. (11) and (12) can be repeated iteratively for a user-specified number of correction cycles. This scheme gives 2nd order accuracy $O(\Delta t^2)$ in time.

4. The controlling oscillatory coastal morphological models

Consider the computing efficiency, stability and accuracy of numerical schemes, we recommend a bed-slope updating, 2 steps with 3-time-levels (2nd order accuracy), WENO morphodynamic scheme (5th order accuracy) to be applied with complex coastal estuary area. The hydraulic modeling system for waves and currents is suggested by Lin et al. (1996), and the sediment transport modeling is suggested by Chiang et al. (1996). It is briefly describe as following. The procedure of the coastal morphological model system is shown as Figure 4.1.

4.1 Coastal morphological system

The bed-slope feedback updating, 2 steps with 3-time-levels, WENO morphological scheme with accuracy $O(\Delta t^2, \Delta x^5, \Delta y^5)$ is shown as below:

Step 1.

$$\frac{z_{bi,j}^{n+1/2} - z_{bi,j}^n}{\Delta t / 2} + \frac{1}{1-n} \frac{\hat{q}_x(q_{x0}, z_{bi}^n)_{i+1/2,j}^n - \hat{q}_x(q_{x0}, z_{bi}^n)_{i-1/2,j}^n}{\Delta x} + \frac{1}{1-n} \frac{\hat{q}_y(q_{y0}, z_{bi}^n)_{i,j+1/2}^n - \hat{q}_y(q_{y0}, z_{bi}^n)_{i,j-1/2}^n}{\Delta y} = 0 \quad (76)$$

Step 2.

$$\frac{z_{bi,j}^{n+1} - z_{bi,j}^n}{\Delta t} + \frac{1}{1-n} \frac{\hat{q}_x(q_{x0}, z_{bi}^{n+1/2})_{i+1/2,j}^{n+1/2} - \hat{q}_x(q_{x0}, z_{bi}^{n+1/2})_{i-1/2,j}^{n+1/2}}{\Delta x} + \frac{1}{1-n} \frac{\hat{q}_y(q_{y0}, z_{bi}^{n+1/2})_{i,j+1/2}^{n+1/2} - \hat{q}_y(q_{y0}, z_{bi}^{n+1/2})_{i,j-1/2}^{n+1/2}}{\Delta y} = 0 \quad (77)$$

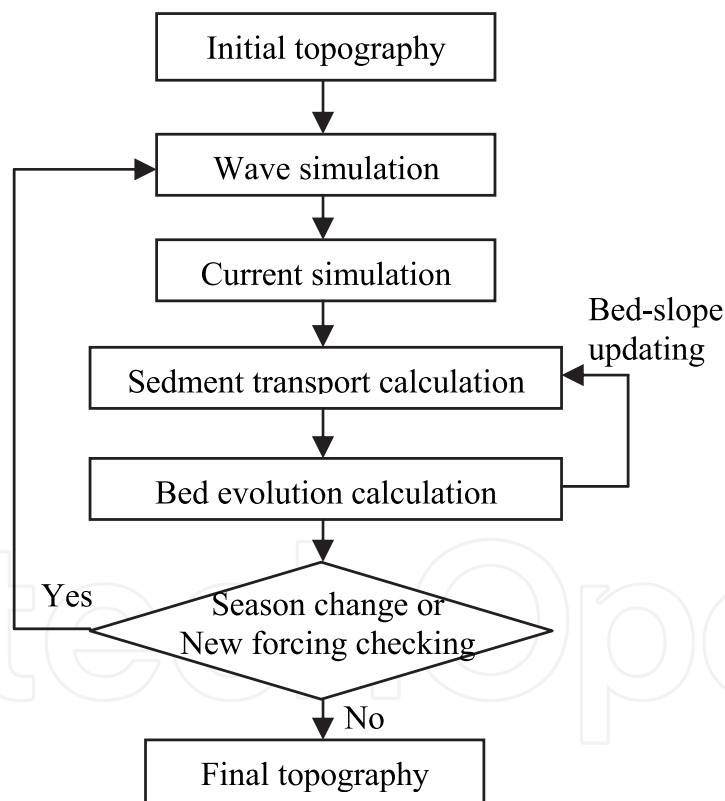


Fig. 4.1 The procedure of the coastal morphological modelling system

4.2 Stability condition analysis

The stability requirement of most morphological schemes is the Courant number $|C_i \Delta t / \Delta x| \leq 1$, and the large Courant numbers observed in the simulation of morphological evolutions suggest that reducing the time steps could improve the stability of the numerical schemes. However, this will increase the computational demand. Fortunately, if the

diffusion terms of Eq. (3) could be properly eliminated, the limit of Courant number could be great than unity. This can be done by carefully giving the values of the diffusivity constants (ε_{xx} , ε_{xy} , ε_{yx} , and ε_{yy}). Some diffusivity constants have been suggested for real coastal environments. Watanabe (1988) suggested that the values are determined empirically through experiments. Struiksmma et al. (1985) and Cayocca (2001) used $\varepsilon_{xx} = \varepsilon_{yy} = 4$, and Kuroiwa and Kamphuis (2003) suggest $\varepsilon_{xx} = \varepsilon_{yy} = 2$. Chiang et al. (2010) recommend $\varepsilon_{xx} = \varepsilon_{yy} = 4$ and $\varepsilon_{xy} = \varepsilon_{yx} = 2$ for complex coastal area. The diffusivity constants were set to $\varepsilon_{xx} = \varepsilon_{yy} = 4$ and $\varepsilon_{xy} = \varepsilon_{yx} = 2$ in following simulation test.

5. Numerical examples and discussions

5.1 Example 1: Miao-Li coastal area in Western Taiwan

5.1.1 Environmental conditions

The developed model is first applied for the complex topography in the Miao-Li county coastal area of western Taiwan. The simulation area (Fig. 5.1) is a sandy beach, which is 7.0 km long in the alongshore direction and 3.5 km wide in the on-off shore direction. This amounts to a maximum depth of around 35.0 m. The median diameter of the beach sand is $d_{50} = 0.25$ mm. The area also has complex beach slopes (from 1/10 to 1/150) and depth contours. The shoreline orientation is in the NNE to NW direction. The tide is semidiurnal with a mean range of around 3.0 m. Since tidal current is negligible in the shore area, waves are the main factors in the coastal dynamics. The dominant wave is the winter northerly monsoon waves between September and March. The significant wave height $H_{1/3}$ is 2.5 m and the significant wave period $T_{1/3}$ is 7.8 sec.

5.1.2 Numerical conditions

In example 5.1, we analyze the morphodynamic evolution results by FTCS (forward time central space), Euler-WENO, and our bed-slope updated 2-step, 3-time-level WENO schemes using the same numerical conditions. The selected sediment coefficients are: $A_1=1.5$ and $A_2=2.5$. The spatial grid sizes of $\Delta x = \Delta y = 10$ m are used in all models (including the sub-models for waves and currents). The time step interval of $\Delta t = 1$ s is used for the nearshore current sub-model and $\Delta t=60$ sec for the morphological model.

5.1.3 Results and discussions

Because we utilize a single directional regular wave to represent all random sea waves, it is very difficult to accurately examine two topography surveys at different times. In order to demonstrate the oscillation removal performance, we compare our results with other schemes that have been reviewed previously. The morphodynamic results after 90 days using the FTCS and Euler-WENO schemes are shown in Figs. 5.2 and 5.3. The results of present morphological scheme after 30, 60, and 90 days are shown in Figs. 5.4, 5.5 and 5.6. We can easily see the significant differences between these three schemes. Present morphological scheme is more stable than the other schemes. As shown in Fig. 5.5, the numerical dispersion, diffusion and oscillations are clearly seen for the FTCS scheme. The results of the Euler-WENO scheme are more stable than FTCS scheme, but the diffusions still occur around -5.0m ~ -2.0m. Similar situations are also found in the wave field and wave-driven current flow field: wave breaking and maximum velocities occur in the same region, which is the steepest area of the beach. The wave breaking and the instability of the

numerical scheme (such as the results of FTCS and Euler-WENO) will cause “shockwaves” in the local area. It is unreasonable for the bed-slope exceeding the rest angle of sand under water. The significance of the bed-slope updating technique and the nonlinear coupling sub-models for morphodynamic system can be clearly identified. This shows that the two-step, three-time-level method can improve the stability in the steep slopes and sharp gradients of beaches in a real coastal area.

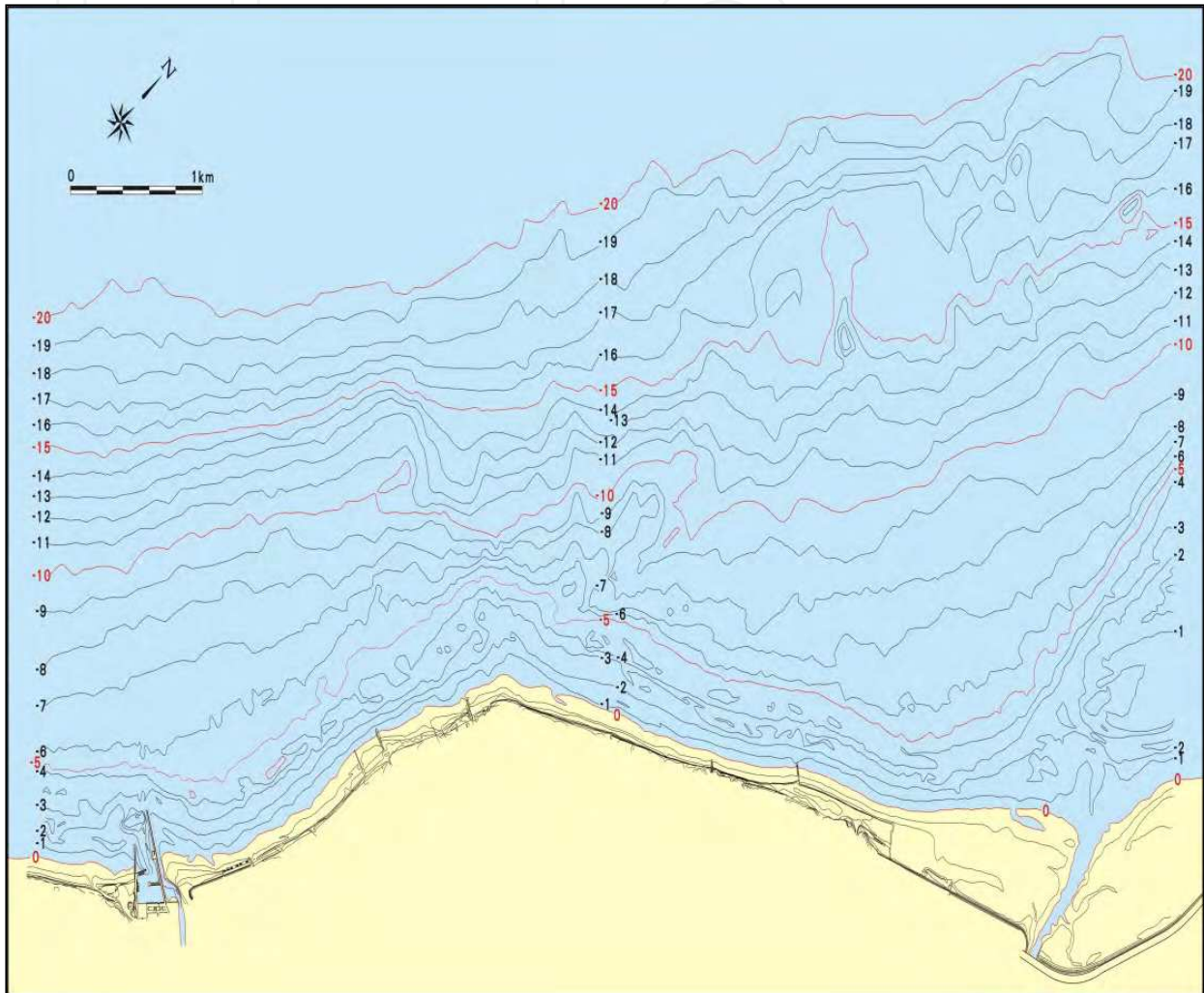


Fig. 5.1 The modeling area of example 1 at Miao-Li county coastal area of western Taiwan.

5.2 Example 2: Tai-Dong coastal area in Eastern Taiwan

In example 2, the Fu-Guon coastal area in Tai-Dong County in eastern Taiwan is considered (Fig. 5.7). The area has a steep and convex topography, which causes wave energy to concentrate. At this site, the tide is semidiurnal with a mean tidal range of less than 1 m. The dominant wave is the summer southern monsoon waves with a significant wave height $H_{1/3} = 1.5$ m and significant wave period $T_{1/3} = 7.0$ sec. The numerical conditions are $A_1=1.7$, $A_2=2.6$. The spatial grid interval is used uniformly with $\Delta x = \Delta y = 5.0$ m in all models (including sub-models of wave and current). The time interval for the nearshore current sub-model is $\Delta t = 1$ s and $\Delta t = 60$ sec for the morphological model.

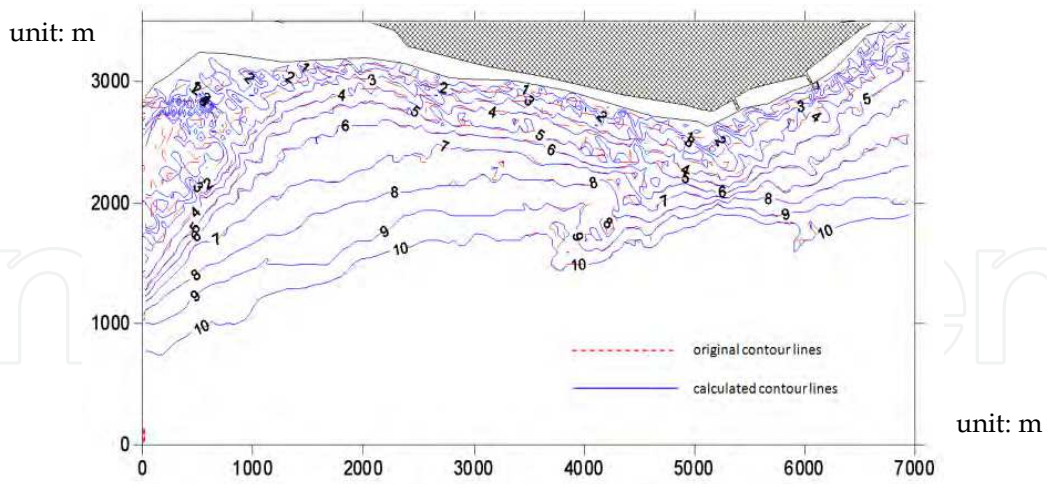


Fig. 5.2 The result of FTCS scheme after 90 days.

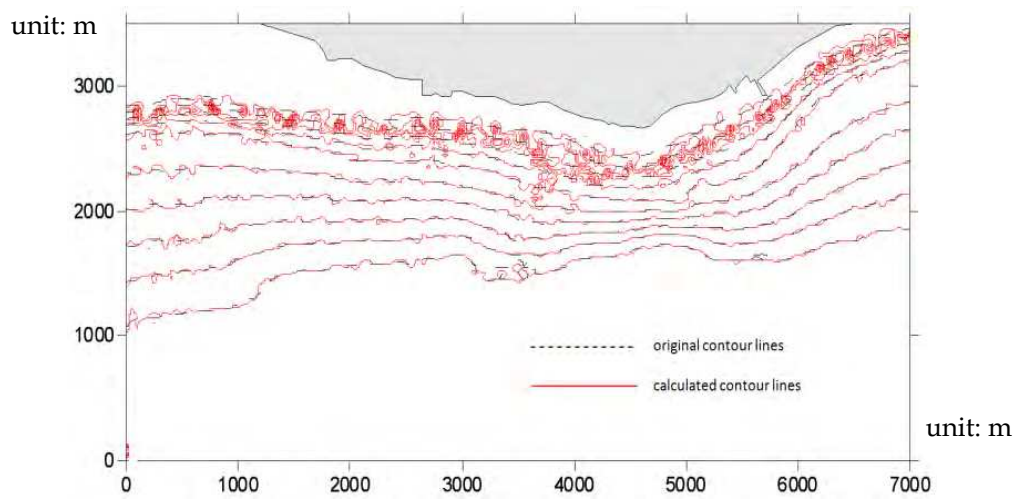


Fig. 5.3 The result of Euler-WENO scheme after 90 days.

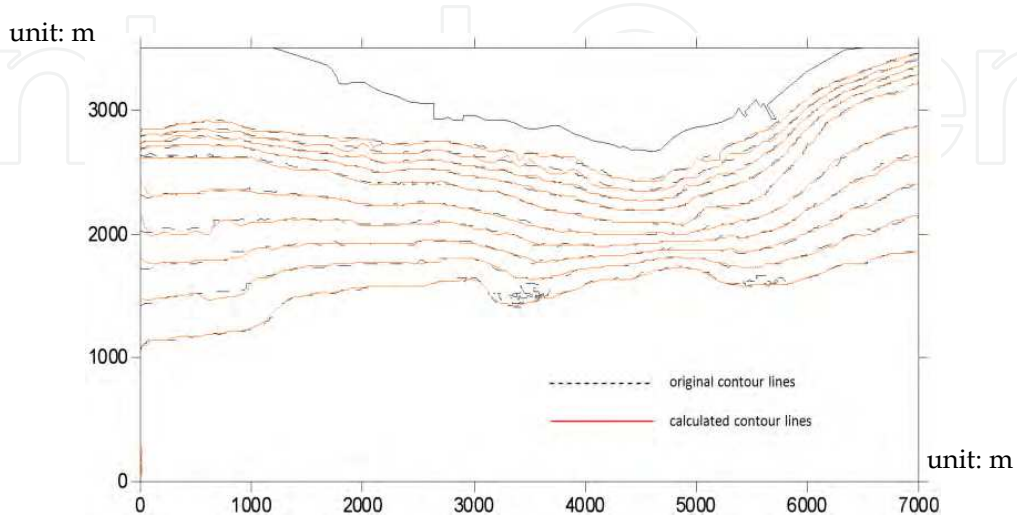


Fig. 5.4 The result of bed-slope updated 2-steps 3-time-levels WENO scheme after 30 days.

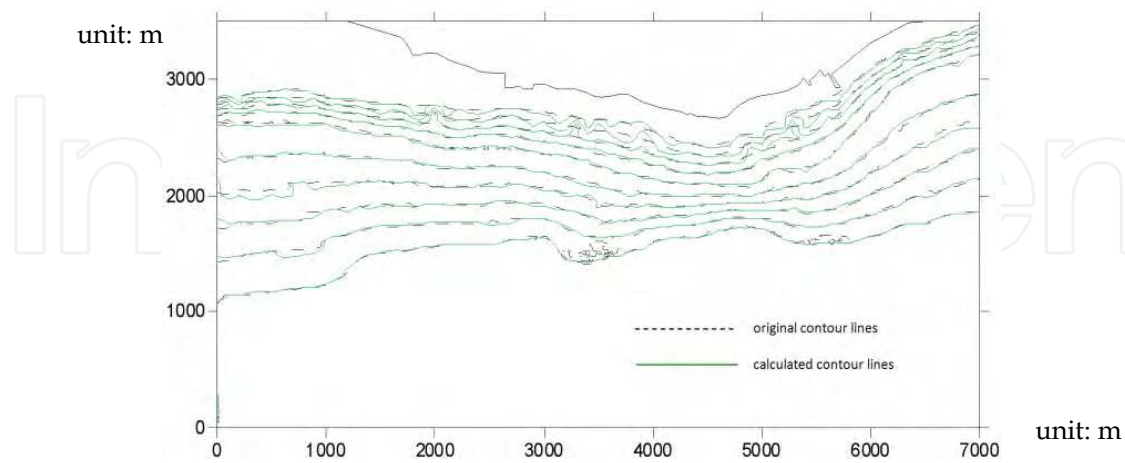


Fig. 5.5 The result of bed-slope updated 2-steps 3-time-levels WENO scheme after 60 days.

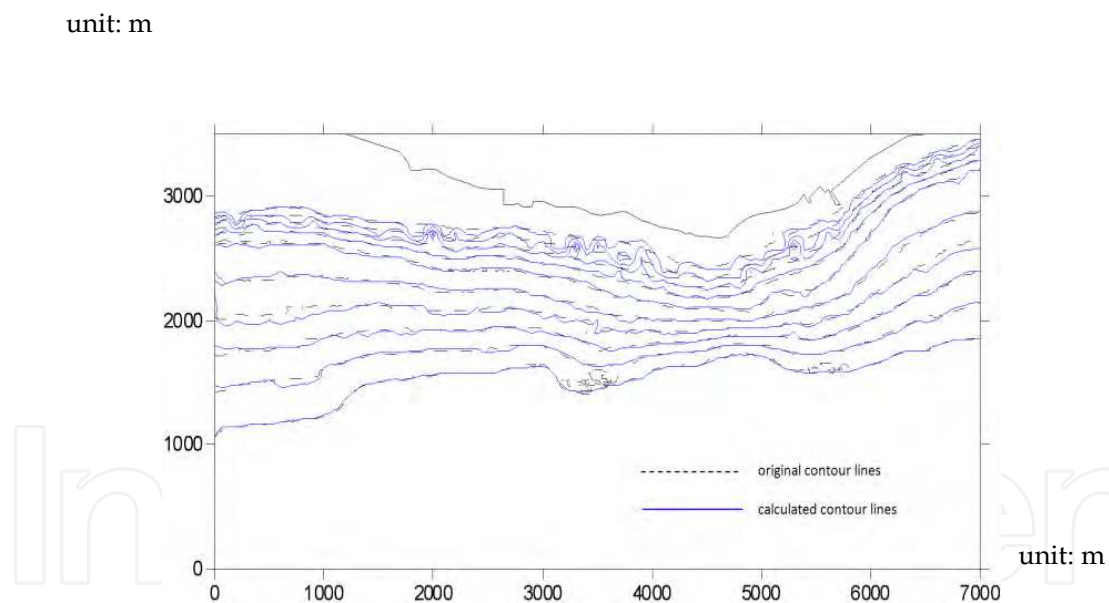


Fig. 5.6 The result of bed-slope updated 2-steps 3-time-levels WENO scheme after 90 days

The morphodynamic results of the Euler-WENO and our schemes are shown in Figs. 5.8 and 5.9. Because of the existence of underwater rigs in this area, the wave energy tends to converge at some locations and diverge at others. Consequently there are oscillations in the numerical simulation of the bed-level evolution, and our schemes are more stable than the others. This can be seen in the topography change results where wave energy was concentrated in Figs. 5.8 and 5.9.

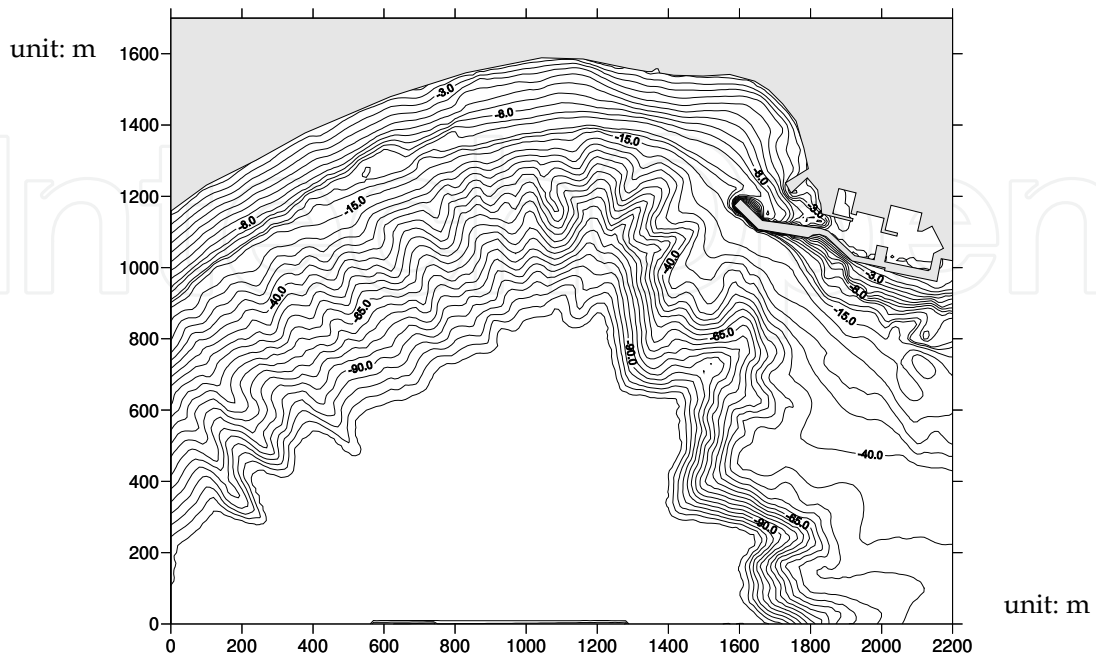


Fig. 5.7 The modeling area of example 2 at Ti-Dong county coastal area of eastern Taiwan.

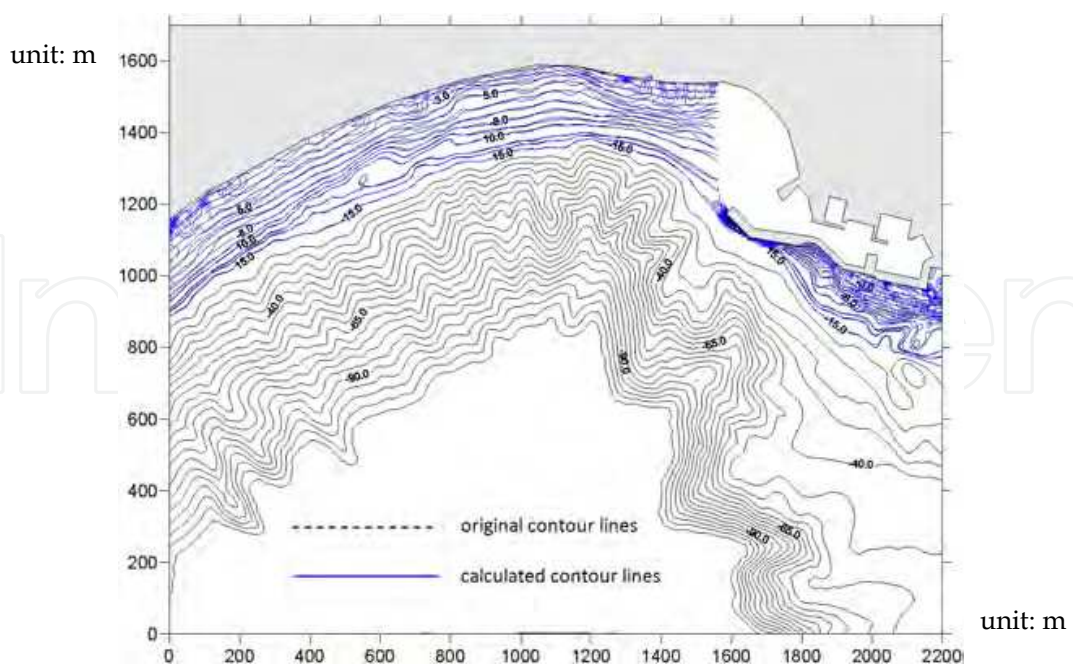


Fig. 5.8 The result of Euler-WENO scheme after 90 days.

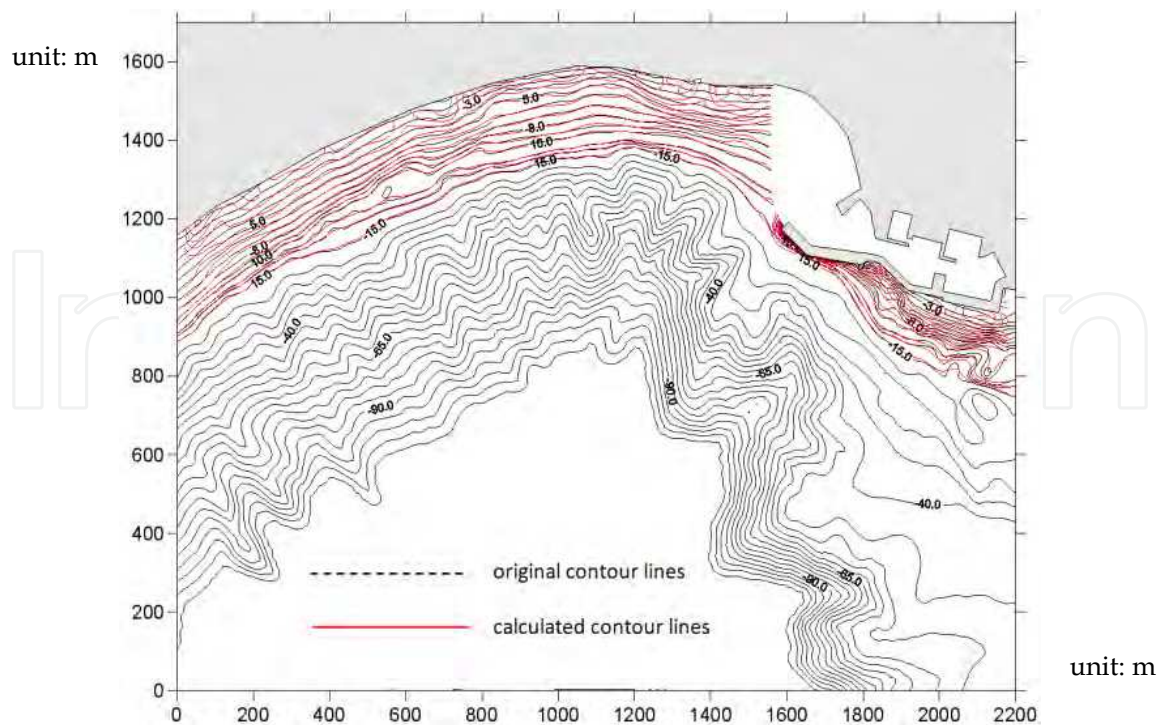


Fig. 5.9 The result of bed-slope updated 2-steps 3-time-levels WENO scheme after 90 days.

6. Conclusion

The evolution of morphodynamic schemes for oscillation removal over the past decade are summarized, the instability of a morphological system is discussed, and numerical solutions of morphodynamic evolution for complex topographies are presented. The bed-slope updated 2-step, 3-time-level WENO scheme has performed well for a real coastal area subject to waves and wave-driven currents. It is sufficiently demonstrated that this scheme provides a significant improvement for shockwave capture and stability in different Δt based on two schematized examples. Results from these two examples suggest the following: the effect of diffusions, dispersions, and oscillations from coupling the sub-models of morphodynamic systems have been improved significantly. The multi-time-level schemes for temporal discretization can improve the stability in examples with steep slopes and sharp gradients of beaches. With carefully selected diffusivity constants, the Courant number can generally exceed unity with reduced time steps efficiently for long-term simulations.

7. References

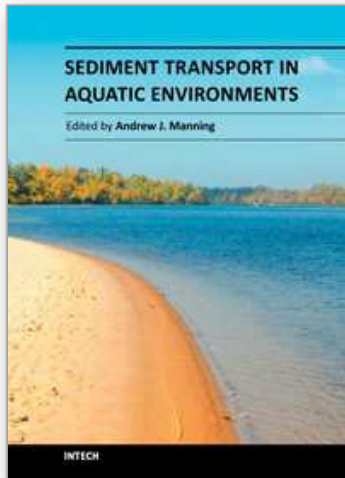
- Andersen, O.H., Hedegaard, I.B., Deigaard, R., de Girolamo, P., Madsen, P., 1991. Model for morphological changes under waves and current, Preprints IAHR, Symposium Suspended Sediment Transport, Florence, Italy, pp. 327-338.
- Antunes Do Carmo, J.S., Seabra-Santos, F.J., 2002. Nearshore sediment dynamics computation under the combined effects of waves and currents, *Advances in Engineering Software*, 33(1), 37-48.

- Callaghan, D. P., Saint-Cast, F., Nielsen, P., Baldock, T. E., 2006. Numerical solutions of the sediment conservation law; a review and improved formulation for coastal morphological modeling, *Coastal Engineering*, 53, 557-571.
- Cayocca, F., 2001. Long-term morphological modeling of a tidal inlet: the Arcachon Basin, France, *Coastal Engineering*, 42(2), 115-142.
- Chiang, Y. C., Lin, M. C., Liou, J. Y., 1996. A Model Formula for Estimation of the Coastal Sediments in West Coast of Taiwan. Proc. 18th Conf. on Ocean Engineering in Republic of China Nov. 1996, pp.619-626.
- Chiang Y.C., Hsiao S.S., Lin M.C., 2010. Numerical solutions of coastal morphodynamic evolution for complex topography. *Journal of Marine Science and Technology*, Vol. 18, No. 3, pp. 333-344.
- Coeffe', Y., Pe'chon, P., 1982. Modelling of sea-bed evolution under wave action. Proceedings 18th Conference ICCE, Capetown.
- de Vriend, H.J., 1987a. 2DH Mathematical modelling of morphological evolution in shallow water. *Coastal Eng.* 11, 1-27.
- de Vriend, H.J., 1987b. Analysis of horizontally two-dimensional morphological evolution in shallow water. *J. Geophys. Res.* 92 _C4., 3877-3893.
- de Vriend, H.J., 1994. Two-dimensional horizontal and weakly three-dimensional models of sediment transport due to waves and currents. In: Abbott, M.B., Price, W.A. Eds., *Coastal, Estuarial and Harbour Engineers' Reference Book*. E&FN. Spon, London, pp. 215-238.
- de Vriend, H.J., Copabianco, M., Chesher, T., De Swart, H.E., Latteux, B., Stive, M.J.F., 1993a. Long term modeling of coastal Morphology. *Coastal Eng.* 21, 225-269.
- de Vriend, H.J., Zyserman, J., Nicholson, J., Roelvink, J.A., Pe'chon, P., Southgate, H.N., 1993b. Medium term 2DH coastal area modeling. *Coastal Eng.* 21, 193-224.
- Harten, A., 1983. High resolution schemes for hyperbolic conservation laws. *J. Comput. Phys.* 49, 357.
- Harten, A., Engquist, B., Osher, S., Chakravarthy, S., 1987. Uniformly high-order accurate essentially non-oscillatory schemes, III. *J. Comput. Phys.* 71, 231. pp. 231-303.
- Henderson, S.M., Allen, J.S., Newberger, P.A., 2004. Nearshore sandbar migration predicted by an eddy-diffusive boundary layer model. *J. Geophys. Res.* 109, C06024. doi:10.1029/2003JC002137.
- Hsu, T.-J., Hanes, D.M., 2004. Effects of wave shape on sheet flow sediment transport. *J. Geophys. Res.* 109, C05025. doi:10.1029/2003JC002075.
- Hudson, J., Damgaard, J., Dodd, N., Chesher, T., Cooper, A., 2005. Numerical approaches for 1D morphodynamic modelling. *Coast. Eng.* 52, 691-707.
- Jensen, J.H., Madsen, E.Ø., Fredsøe, J., 1999. Oblique flowover dredged channels: II. Sediment transport and morphology. *J. of Hydraul. Eng.* 125 (11),1190-1198.
- Jiang, G.-S., Shu, C.-W., 1996. Efficient implementation of weighted ENO schemes. *J. Comput. Phys.* 126, 202.
- Jiang, G.-S., Wu, C.-C., 1999. A high-order WENO finite difference scheme for the equations of ideal magnetohydrodynamics. *J. Comput. Phys.* 150, 561-594.
- Jiang, G.-S., Levy, D., Lin, C.-T., Osher, S., Tadmor, E., 1998. High-resolution nonoscillatory central schemes with nonstaggered grids for hyperbolic conservation laws. *SIAM Journal on Numerical Analysis* 35 (6), 2147-2168.

- Johnson, H.K., Zyserman, J.A., 2002. Controlling spatial oscillations in bed level update schemes. *Coast. Eng.* 46, 109–126.
- Lin, M. C., Kuo, J. C., Chiang, Y. C., Liou, J. Y., 1996. Numerical Modeling of Topography Changes in Sea Region. *Proc. 18th Conf. on Ocean Engineering in Republic of China Nov. 1996*, pp.627-637.
- Liu, X.-D., Osher, S., Chan, T., 1994. Weighted essentially non-oscillatory schemes. *J. Comput. Phys.* 115, 200.
- Long, W., Kirby, J. T., Shao Z., 2008. A numerical scheme for morphological bed level calculations, *Coastal Engineering*, Vol. 55 167–180 .
- Maruyama, K., Takagi, T., 1988. A simulation system of nearshore sediment transport for the coupling of the sea-bottom topography, waves and currents. *Proc. IAHR, Copenhagen*.
- Nicholson, J., Broker, I., Roelvink, J.A., Price, D., Tanguy, J.M., Moreno, L., 1997. Intercomparison of coastal area morphodynamic models. *Coast. Eng.* 31, 97–123.
- Nairn, R.B., Southgate, H.N., 1993. Deterministic profile modelling of nearshore processes. Part 2. Sediment transport and beach profile development. *Coastal Engineering* 19 (1-2), 57–96.
- O'Connor, B.A., Nicholson, J., 1989. Modelling changes in coastal morphology, *Sediment Transport Modeling*. In: Wang, S.S.Y. (Ed.), ASCE, pp. 160–165.
- Roelvink, J.A., van Banning, G.K.F.M., 1994. Design and development of Delft3D and application to coastal morphodynamics. In: Verwey, Minns, Babovic, Maksimovic (Eds.), *Hydroinformatics '94*. Balkema, Rotterdam, pp. 451–455.
- Roelvink, J.A., Walstra, D.J.R., Chen, Z., 1998. Morphological modelling of Keta lagoon case. *Proc. 24th Int. Conf. on Coastal Engineering*. ASCE, Kobe, Japan.
- Roelvink, J.A., 2006. Coastal morphodynamic evolution techniques. *Coast. Eng.* 53, 277–287.
- Saint-Cast, F., 2002. *Modelisation de la morphodynamique des corps sableux en milieu littoral (Modelling of Coastal Sand Banks Morphodynamics)*. University Bordeaux I, Bordeaux. 245 pp.
- Saint-Cast, F., Caltagirone, J.P., Bonneton, P., 2001. On the splitting of the sediment fluxes balance: a new formulation for the sand waves equation. *Coastal Engineering 2001, Computer Modelling of Seas and Coastal Regions, Rhodes, Greece*, pp. 2–12.
- Sato, K., Shuto, N., Tanaka, H., 1995, Numerical simulation of the sand spit flushing at a river mouth. In: *Chinese Hydraulic Engineering Society and International Research and Training Center on Erosion and Sedimentation (Ed.)*, *Adv. In Hydro-Science and Eng.*, vol. II, Part B, Tsinghua University Press, Beijing, pp. 1399-1406.
- Shao, Z.Y., Kim, S., Yost, S.A., 2004. A portable numerical method for flow with discontinuities and shocks. *Proceedings of 17th Engineering Mechanics Conference, ASCE, June 13-16. Paper*, vol. 65. University of Delaware, Newark, DE, USA (on CD).
- Shu, C.-W., 1997, Essentially non-oscillatory and weighted essentially non-oscillatory schemes for hyperbolic conservation laws, lecture notes. ICASE Report No. 97-65, NASA/CR-97-206253. November.
- Shu, C.-W., Osher, S., 1988. Efficient implementation of essentially non-oscillatory shock-capturing schemes. *J. Comput. Phys.* 77, 439–471.

- Struiksma, N., Olewesen, K.W., Flokstra, C., de Vriend, H.J., 1985. Bed deformation in curved alluvial channels. *J. Hydraul. Res.* 23 (1).
- Vincent, S., Caltagirone, J.P., 1999. Efficient solving method for unsteady incompressible interfacial flow problems. *International Journal For Numerical Methods In Fluids* 30 (6), 795-811.
- Wang, Z.B., 1992. Theoretical analysis on depth-integrated modeling of suspended sediment transport. *J. Hydrol. Res.* 30 (3).
- Watanabe, A., 1982. Numerical models of near-shore currents and beach deformation. *Coastal Eng., Jpn.* 25, 147-161.
- Watanabe, A., Maruyama, K., Shimizu, T., Sakakiyama, T., 1986. Numerical prediction model of three-dimensional beach deformation around a structure. *Coastal Eng., Jpn.* 29.
- Watanabe, A., 1988, Modeling of sediment and beach evolution. In: Horikawa, K. (Ed.), *Nearshore Dynamics and Coastal Processes*. University of Tokyo Press, Tokyo, Japan, pp. 292-302.
- Yamaguchi M., Nishioka Y., 1984, Numerical simulation on the change of bottom topography by the presence of coastal structures, *Proc. 19th Int. Conf. on Coastal Engineering*, ASCE, Houston, pp. 1732-1748.

IntechOpen



Sediment Transport in Aquatic Environments

Edited by Dr. Andrew Manning

ISBN 978-953-307-586-0

Hard cover, 332 pages

Publisher InTech

Published online 30, September, 2011

Published in print edition September, 2011

Sediment Transport in Aquatic Environments is a book which covers a wide range of topics. The effective management of many aquatic environments, requires a detailed understanding of sediment dynamics. This has both environmental and economic implications, especially where there is any anthropogenic involvement. Numerical models are often the tool used for predicting the transport and fate of sediment movement in these situations, as they can estimate the various spatial and temporal fluxes. However, the physical sedimentary processes can vary quite considerably depending upon whether the local sediments are fully cohesive, non-cohesive, or a mixture of both types. For this reason for more than half a century, scientists, engineers, hydrologists and mathematicians have all been continuing to conduct research into the many aspects which influence sediment transport. These issues range from processes such as erosion and deposition to how sediment process observations can be applied in sediment transport modeling frameworks. This book reports the findings from recent research in applied sediment transport which has been conducted in a wide range of aquatic environments. The research was carried out by researchers who specialize in the transport of sediments and related issues. I highly recommend this textbook to both scientists and engineers who deal with sediment transport issues.

How to reference

In order to correctly reference this scholarly work, feel free to copy and paste the following:

Yun-Chih Chiang and Sung-Shang Hsiao (2011). Coastal Morphological Modeling, Sediment Transport in Aquatic Environments, Dr. Andrew Manning (Ed.), ISBN: 978-953-307-586-0, InTech, Available from: <http://www.intechopen.com/books/sediment-transport-in-aquatic-environments/coastal-morphological-modeling>

INTECH
open science | open minds

InTech Europe

University Campus STeP Ri
Slavka Krautzeka 83/A
51000 Rijeka, Croatia
Phone: +385 (51) 770 447
Fax: +385 (51) 686 166
www.intechopen.com

InTech China

Unit 405, Office Block, Hotel Equatorial Shanghai
No.65, Yan An Road (West), Shanghai, 200040, China
中国上海市延安西路65号上海国际贵都大饭店办公楼405单元
Phone: +86-21-62489820
Fax: +86-21-62489821

© 2011 The Author(s). Licensee IntechOpen. This chapter is distributed under the terms of the [Creative Commons Attribution-NonCommercial-ShareAlike-3.0 License](#), which permits use, distribution and reproduction for non-commercial purposes, provided the original is properly cited and derivative works building on this content are distributed under the same license.

IntechOpen

IntechOpen